LAWRENCE
LIVERMORE
NATIONAL
LABORATORY

LLNL-JRNL-406614

On the microstructure of nanoporous gold: an x-ray diffraction study

S. Van Petegem, S. Brandstetter, R. Maaß, B. Schmitt, C. Borca, H. Van Swygenhoven, A. M. Hodge, B. S. El-Dasher, J. Biener

August 28, 2008

Nanoletters

Disclaimer

On the microstructure of nanoporous gold: an x-ray diffraction study

Steven Van Petegem[1], *Stefan Brandstetter*[1], *Robert Maaß*[1], *Bernd Schmitt*[1], *Camelia Borca*[1], *Helena Van Swygenhoven*[1,*],

Andrea M. Hodge[2,#], *Bassem S. El-Dasher*[2], *Jürgen Biener*[2]

[1]Paul Scherrer Institut, CH-5232 Villigen, Switzerland

[2]Nanoscale Synthesis and Characterization Laboratory, Lawrence Livermore National Laboratory, Livermore, CA 94551-9900, USA

*Corresponding author: helena.vanswygenhoven@psi.ch

#now at: Aerospace and Mechanical Engineering Department, University of Southern California, Los Angeles, 90089, USA

The evolution of the grain structure, internal stresses, and the lattice misorientations of nanoporous gold (npAu) during dealloying of bulk (3D) Ag-Au alloy samples was studied by various in-situ and ex-situ X-ray diffraction techniques including powder and Laue diffraction. The experiments reveal that the dealloying process preserves the original crystallographic structure, but leads to a small spread in orientations within individual grains. Furthermore, most grains develop in-plane tensile stress. The feature size of the developing nanoporous structure increases with increasing dealloying time.

Recently, nanoporous gold (np-Au) has attracted considerable attention fueled by its interesting mechanical properties[1,2] and its possible use in actuator[3], sensor[4,5,6], and catalysis[7] applications. The material can be easily prepared from Ag-Au alloys of suitable composition (e.g. $Au_{0.3}Ag_{0.7}$) by using a simple dealloying process, and exhibits a characteristic sponge-like structure with a unimodal pore size distribution on the nanometer length scale[8,9,10] Although large progress has been made in understanding the fundamentals of the dealloying process[8,11,12,13] there are still aspects which need to be addressed such as what happens to the microstructure of np-Au during dealloying. Current models assume that dealloying can be described by simple dissolution and diffusion processes on a rigid lattice without considering phenomena such as recrystallization or stress induced plastic deformation[8]. However, the observation that dealloying of Ag-Au alloys can lead to macroscopic sample shrinkage of up to 30% clearly demonstrates that plastic deformation during dealloying needs to be considered[14]. Indeed, surface stress induced yielding of Au nanowires with diameters of a few nanometer (which most likely are being formed as intermediates during dealloying[12]) has been observed in atomistic simulations[15]. This immediately raises the question if, and to what extent, the microstructure of the Ag-Au starting alloy is preserved during dealloying, or if the grain structure is modified for example by stress-driven mechanical deformation. This is an important issue as changes in the microstructure can be expected to affect both the mechanical[16] and catalytic properties of nanoporous gold[17,18,19] The existing experimental evidence is controversial: On one hand, dealloying experiments performed on ~100 nm thin Au-Ag alloy films suggest that the crystal microstructure does not change dramatically during dealloying but also revealed the formation of strain inhomogeneities and/or defects[9]. On the other hand, transmission electron microscopy (TEM) micrographs of np-Au samples prepared from bulk (several hundred micron thick) samples of np-Au showed a nanocrystalline grain structure[20]. The question is whether these controversial results are real and reflect different experimental conditions (for example

2D versus 3D samples), or are an artifact of the TEM sample preparation in case of 3D samples. For example, it is known that TEM sample preparation techniques such as microtome slicing and focused ion beam (FIB) milling can introduce surface relaxation and/or severe damage[21,22]. On the other hand, a 100-nm-thick sample is certainly a more compliant substrate than a thick 3D sample which should help to relieve the stresses developing at the dealloying front thus preventing plastic deformation to occur.

In this work, we addressed the questions raised above by performing time-resolved *in situ* x-ray diffraction experiments during dealloying of Ag-Au alloys followed up by a set of *ex situ* microstructural characterization experiments including x-ray microdiffraction. X-ray diffraction has the advantage of being a non-destructive technique capable of providing detailed information about the microstructure of 3D samples including grain size, lattice constant and strains. Previous *in situ* x-ray diffraction studies on dealloying provided crucial information on the early stages of the dealloying process[23,24,25] but did not address the formation of the 3D nanoporous structure. In this study we focus on the evolving microstructure in particular addressing the evolving internal stresses during dealloying and the lattice misorientations previously observed in TEM.

A polycrystalline $Au_{30}Ag_{70}$ alloy ingot was prepared by melting Au (99.999 %) and Ag (99.999 %) at 1100 °C and homogenizing the material for 70 hrs at 875 °C under an argon atmosphere. For the x-ray measurements ~50 μm thin strips were cut, polished and then heat-treated for 8 hrs at 800 °C to relieve stress. The *in situ* x-ray experiments were performed at the powder diffraction station of the Materials Science beamline at the Swiss Light Source (SLS) in Switzerland. Figure 1 shows a schematic view of the setup. The AgAu samples with a thickness of about 50 μm are positioned in an Al sample holder and immersed in nitric acid in a standard Pyrex container. The bottom of the container is thinned to a

thickness of 100 μm in order to reduce the background scattering arising from the amorphous Pyrex structure. In order to avoid tensile stress build up during dealloying because of sample shrinkage (see e.g. Refs. [14,26]) the samples are allowed to move in lateral direction. The incoming x-ray beam had a size of approximately 500×500μm^2. In order to penetrate both the dissolving liquid and the specimen an x-ray energy of 30keV was chosen. The diffracted beam is recorded in reflection mode by the Mythen microstrip detector. The current version of this detector allows recording a full 120° x-ray diffraction pattern in a few seconds with negligible readout time. Note that in this geometry the angle between the incoming beam and the sample is fixed during the experiment[27].

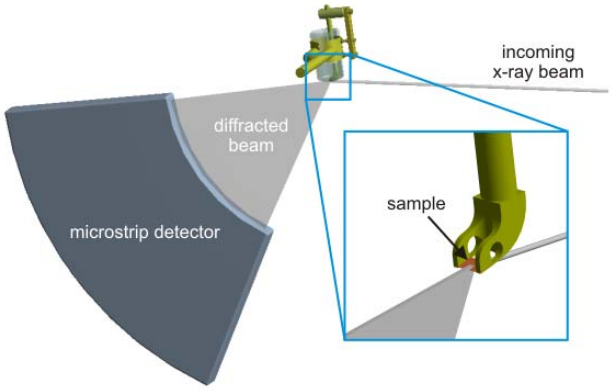

Figure 1. Schematic view of the *in situ* setup.

The *in situ* experiments are complemented by conventional x-ray diffraction, x-ray micro-diffraction and microscopy observations. The conventional x-ray measurements were performed in Bragg-Brentano geometry on a Siemens D500 laboratory diffractometer equipped with a Cu anode. The microdiffraction experiments were performed at the MicroXAS beamline of the Swiss Light Source. Here, the x-ray beam was focused to a size of 4×3μm^2 and 1×1μm^2 for, respectively, monochromatic (11.5 keV) and polychromatic (5-23 keV) light. The diffracted signal is recorded by a large two dimensional CCD detector in transmission geometry. For the Laue patterns the diffraction peaks were

identified using an automatic indexation routine using an approach similar as described in Ref. [28]. The positions of the diffraction spots in a Laue pattern can be used to determine the local crystallographic orientation, similar to EBSD but with a much better resolution. Collecting Laue diffraction patterns at several positions within a single grain therefore allows one to identify rotational components.

Several *in situ* experiments were performed during which $Au_{30}Ag_{70}$ samples were immersed in nitric acid for several hours (free corrosion). Morphology (ligament size) and composition (amount of residual Ag) were assessed by cross-sectional Scanning Electron Microscopy (SEM) and Energy Dispersive Spectroscopy (EDAX). The SEM micrograph shown in Figure 2 was collected from a sample which was dealloyed for 4h, and reveals the formation of a nanoporous microstructure with an average ligament size of 31±5nm. The concentration of residual Ag in this sample was found to be less than one percent throughout the cross section indicating that the dealloying process was completed.

Electron backscatter diffraction (EBSD) inverse pole figure maps collected from the same sample area before and after dealloying are displayed in Figure 3. The $Au_{30}Ag_{70}$ alloy exhibits a broad grain size distribution with grain sizes ranging from a few up to hundreds of micrometers. Note that the EBSD inverse pole figure maps suggest that both grain morphology and orientation are preserved during the dealloying process. On the other hand, cross-sectional TEM micrographs collected from the same area (using a FIB lit-out technique) indicted the formation of a textured nanocrystalline microstructure similar to that reported from microtomed cross sections of np-Au[20]. As we will show in the following, the observation of a nanocrystalline grain structure in cross sectional TEM samples seems to be an artifact of the TEM sample preparation.

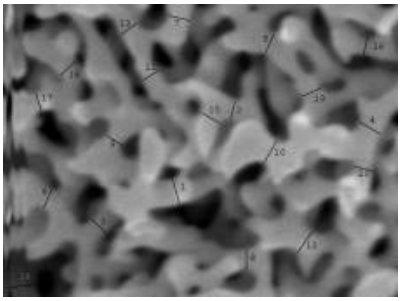

Figure 2. SEM image of the final nanoporous structure.

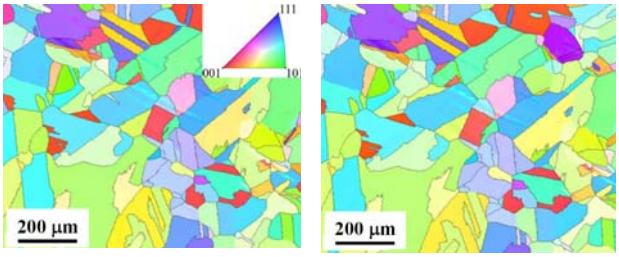

Figure 3. Electron backscatter diffraction (EBSD) inverse pole figure maps (1100 x 900 µm^2, step size was 2.5µm) showing the grain structure and orientation before (left) and after (right) dealloying.

Figure 4 displays a typical x-ray diffraction pattern of the initial $Au_{30}Ag_{70}$ alloy recorded with the *in situ* setup. The spectrum is characterized by large intensity variations among the diffraction peaks, which indicates that only a limited number of grains is illuminated consistent with the coarse-grained structure of our starting alloy. By varying the angle of the incoming beam different grains are fulfilling the diffraction conditions, resulting in a different set of high intensity peaks. This is an indication that most diffraction peaks originate from a single grain. For all *in situ* experiments this angle was chosen such that the spectrum contained at least three diffraction peaks with reasonable intensity. The diffraction peaks did not exhibit any size and/or strain broadening indicating a relaxed large-grained microstructure of our Au-Ag starting alloy.

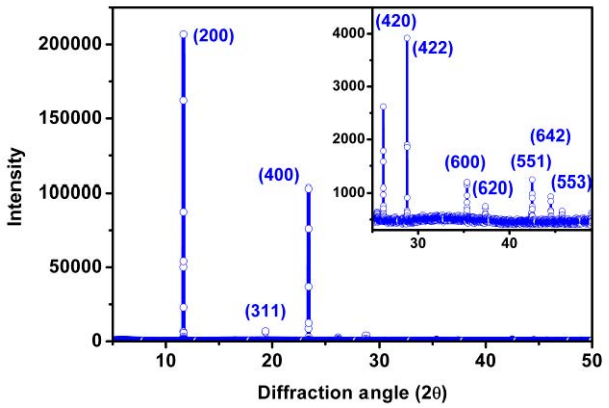

Figure 4. X-ray diffraction pattern of a $Au_{30}Ag_{70}$ sample before dealloying. The pattern for diffraction angles between 25° and 50° is shown in more detail in the inset.

The evolution of the (311) diffraction peak as function of dealloying time is shown in Figure 5. After a few minutes a very broad peak appears under the original narrow peak. This broad feature can be attributed to the formation of np-Au. Its intensity continuously increases at the expense of the intensity of the narrow diffraction peak. After about 30 minutes the original diffraction peak has completely disappeared and only the contribution of nanoporous gold is left. A qualitative similar behavior is observed for the other diffraction peaks. Furthermore, no new diffraction peaks appear during dealloying, with other words, the spectrum does not evolve to a powder diffraction spectrum. This observation reveals that the original crystal structure is retained during dealloying, consistent with the EBSD result shown in figure 3.

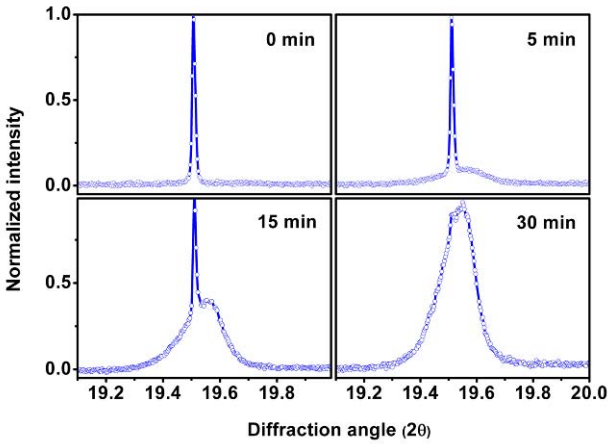

Figure 5. The (311) diffraction peak as function of dealloying time. The maximum intensity is normalized to 1.

The diffraction peaks were fitted with a split PearsonVII function. The evolution of the full-width at half-maximum (FWHM) of the broad component of the (311) and (400) diffraction peaks is displayed in figure 6. A smooth decrease of the FWHM during dealloying is observed. This decrease is similar for all diffraction peaks and extends far beyond the completion of the Ag dissolution of this particular grain thus indicating that the feature size in np-Au increases continuously with time while being in contact with nitric acid. This coarsening is confirmed by SEM micrographs collected from a specimen that was dealloyed for only 0.5h which leads to an average ligament size of ~15nm. Similar observations have also been reported by Newman and Sieradzki. using *in situ* small angle neutron scattering[12]. The coarsening of np-Au can be explained by curvature-driven surface diffusion which is assisted by the high mobility of gold atoms at the liquid-gold interface. No clear indication for strain relaxation could be found.

A conventional *ex situ* x-ray spectrum of the dealloyed sample was recorded with a large beam size that covers the entire sample. Here all diffraction peaks are present. Using a conventional Williamson-

Hall analysis method we find a coherent scattering length of 30 nm (consistent with our SEM observation) and a root-mean-square strain of 0.09%. This relatively small strain value is consistent with the mechanical robustness of our material despite the general brittleness of np-Au[29].

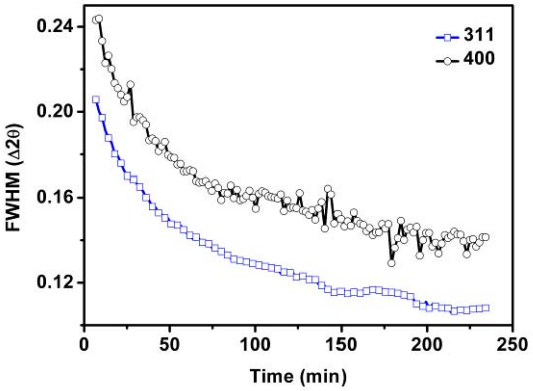

Figure 6. Evolution of the FWHM of the (311) and (400) peak as function of dealloying time.

To obtain more detailed information about the microstructure of the ligaments x-ray microdiffraction experiments were performed on the samples after dealloying. Two-dimensional diffraction patterns are recorded with a micron sized beam which is focused on a small volume within a single grain. Figure 7 displays a representative two-dimensional diffraction spectrum obtained with a monochromatic beam. It contains one high intensity broad diffraction spot with an approximately axisymmetric shape. For most grains, the positions of the diffraction spots reveal significant in-plane tensile strains. A few, however, are found to exhibit compressive strain.

Laue diffraction experiments were performed at various positions inside single grains, usually illuminating one or at most two grains. For all probed grains small but measurable lattice misorientations are observed. This is demonstrated in figure 8 showing the angular change in crystallographic directions parallel and perpendicular to the beam direction during a line scan in a 70

μm grain. In this particular grain the crystal lattice mainly rotates around a direction parallel to the sample surface. Additionally, twins were found in several grains.

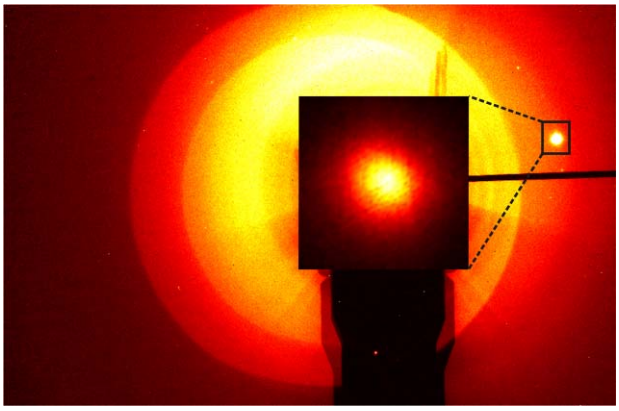

Figure 7. Typical two-dimensional microdiffraction pattern of nanoporous gold obtained with a monochromatic beam.

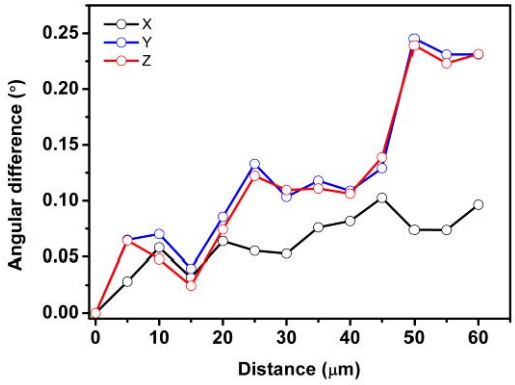

Figure 8. Relative change of the local crystal orientation within a grain. Z denotes the beam direction. X and Y are the horizontal and vertical in-plane directions, respectively.

The in and ex situ x-ray diffraction experiments reported here provide essential information on microstructural details of the nanoporous structure. The in situ x-ray measurements show that the microstructure of the original AgAu alloy is predominantly preserved, in contrast to our previous TEM

observations. In particular, the development of new grain boundaries during dealloying was not observed as evidenced by the absence of rings (fully random granular structure) or parts of rings (textured structure) in our monochromatic x-ray microdiffraction experiments. In none of the probed grains evidence for such a granular structure could be found. On the contrary, all Laue diffraction patterns indicate the presence of at most two grains in the illuminated volume. However, we found evidence for small lattice misorientations within a grain (fig.8). The preservation of the original grain structure results in a non-relaxed microstructure with an rms-strain of about 0.1%, which is of the same order of magnitude as observed in some nanocrystalline materials with similar grain size. These rms-strains can originate from microstructural defects such as dislocations, or from inter- and intragranular stress variations.

In order to address in more detail the origin of the nanocrystalline structure reported after dealloying (Ref. 20) we investigated the influence of FIB damage on a nanoporous structure. Micron-sized pillars produced by FIB milling were investigated using microdiffraction. Pillars with a diameter of 4μm and aspect ratio of 2.3 were produced by perpendicular FIB milling using a two-step procedure similar to the one described in Ref.s [2,30]. The pillars are positioned with micrometer precision in the x-ray beam using a fluorescence mapping technique[31]. The orientation of the pillars' vertical axes is determined to ~[2 3 9] by white beam Laue diffraction and the Laue patterns also disclose a (-1-11) twin contribution. Figure 9 displays a two-dimensional x-ray microdiffraction image taken with a monochromatic beam (11.5keV) in the center of one of the pillars. Note the observation of several diffraction peaks in contrast to the typical microdiffraction pattern obtained from the original nanoporous structure (Figure 7). All peaks exhibit heavy azimuthal streaking indicating the presence of an orientation distribution of about 10-15 degrees on the indexed (111), (200) and (220) Debye rings.

This is in agreement with the highly textured nanocrystalline structure observed in nanoporous TEM lamella produced by microtoming[20] or the FIB lift-out technique. Note that in this image the central part of the pillar, which is presumably not influenced by FIB damage and thus still single crystalline, is not in diffraction conditions and therefore not contributing to the diffraction pattern. The multiple ring segments, for instance on the (111) ring, presumably originate from the outer FIB damaged layer. The width of the diffraction peaks in radial direction is slightly narrower than expected, indicating possible ligament growth due to FIB milling, in agreement with observations by Sun and Balk[21].

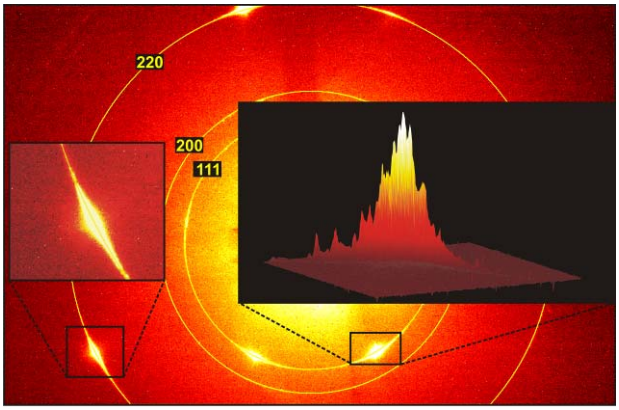

Figure 9. 2D x-ray microdiffraction image of a nanoporous gold pillar. The inset displays a 3D image of a part of the (111) ring.

In conclusion, dealloying of bulk Ag-Au alloy samples by free corrosion results in the formation of a nanoporous structure that has a similar grain morphology and orientation as the original alloy sample. The grains exhibit a small spread in crystal orientation and often in-plane tensile stresses are observed, resulting in an rms strain of 0.1%. The presence of tensile stress is expected to negatively affect the mechanical robustness of this brittle material, and may also affect the catalytic properties of npAu. Standard TEM sample preparation techniques such as microtoming and FIB lift-out were found to lead to severe plastic deformation resulting in an apparent nanocrystalline grain structure.

Acknowledgement. The authors thank D. Grolimund and M. Willimann from the MicroXAS beam line at the Swiss Light Source for technical support and C.A. Volkert for providing the nanoporous gold micropillars. HVS thanks the Swiss National Science Foundation and the European Commission (6^{th} Framework) for financial support of the project NANOMESO. Part of this work was performed under the auspices of the U.S. Department of Energy by Lawrence Livermore National Laboratory under contract DE-AC52-07NA27344.

[1] J. Biener, A. M. Hodge, J. R. Hayes, C. A. Volkert, L. A. Zepeda-Ruiz, A. V. Hamza, and F. F. Abraham, *Nano Lett.* **2006**, 6**,** 2379.

[2] C. A. Volkert, E. T. Lilleodden, D. Kramer, and J. Weissmuller, *Appl. Phys. Lett.* **2006**, 89**,** 061920

[3] Kramer, D.; Viswanath, R. N.; Weissmueller, J. *Nano Lett.* **2004**, *4*, 793-796.

[4] J. Biener, G. W. Nyce, A. M. Hodge, M. M. Biener, A. V. Hamza, and S. A. Maier, *Adv. Mater.* **2008**, 20**,** 1211

[5] Bonroy, K.; Friedt, J.-M.; Frederix, F.; Laureyn, W.; Langerock, S.; Campitelli, A.; Sara, M.; Borghs, G.; Goddeeris, B.; Declerck, P. *Anal. Chem.* **2004**, *76*, 4299-4306.

[6] Hieda, M.; Garcia, R.; Dixon, M.; Daniel, T.; Allara, D.; Chan, M. H. W. *Appl. Phys. Lett.* **2004**, *84*, 628-630.

[7] V. Zielasek, B. Jurgens, C. Schulz, J. Biener, M. M. Biener, A. V. Hamza, and M. Baumer, *Angew. Chem. Int. Ed.* **2006**, 45**,** 8241

[8] J. Erlebacher, M.J. Aziz, A. Karma, N. Dimitrov, K. Sieradzki, Nature **2001**, 410, 450.

[9] H. Roesner, S. Parida, D. Kramer, C. A. Volkert, and J. Weissmueller, *Adv. Eng. Mater.* **2007**, 9**,** 535

[10] T. Fujita, L. H. Qian, K. Inoke, J. Erlebacher, and M. W. Chen, *Appl. Phys. Lett.* **2008**, 92**,** 251902.

[11] J. Erlebacher, K. Sieradzki, Scripta Mater. **2003**, 49, 991.

[12] R. C. Newman and K. Sieradzki, *Mrs Bulletin* **1999**, 24**,** 12.

[13] J. Erlebacher, J. Electrochem. Soc. **2004**, 151, C614.

[14] S. Parida, D. Kramer, C.A. Volkert, H. Rosner, J. Erlebacher, J. Weissmuller, Phys. Rev. Lett. **2006**, 97, 035504.

[15] J. K. Diao, K. Gall, M. L. Dunn, and J. A. Zimmerman, *Acta Mater.* **2006**, 54**,** 643.

[16] A. M. Hodge, J. Biener, L. L. Hsiung, Y. M. Wang, A. V. Hamza, and J. H. Satcher, *J. Mater. Res.* **2005**, 20**,** 554.

[17] M. Mavrikakis, B. Hammer, J.K. Nørskov, Phys. Rev. Lett. **1998**, 81, 2819

[18] M. Gsell, P. Jacob, D. Menzel, Science **1998**, 280, 717

[19] M. Mavrikakis, P. Stoltze, J.K. Nørskov, Catal. Lett. **2000**, 64, 101

[20] J. Biener, A. M. Hodge, A. V. Hamza, L. M. Hsiung, and J. H. Satcher, *Journal of Applied Physics* **2005**, 97**,** 024301

[21] Y. Sun and T.J. Balk, Scripta Mater. **2008**, 58, 727

[22] J. Mayer, L. A. Giannuzzi, T. Kamino, J. Michael, MRS Bulletin **2007**, 32, 400

[23] F.U. Renner, A. Stierle, H. Dosch, D.M. Kolb, T.-L. Lee, J. Zegenhagen, Nature **2006**, 439, 707

[24] F.U. Renner, A. Stierle, H. Dosch, D.M. Kolb, J. Zegenhagen, Electrochem. Comm. **2007**, 9, 1639

[25] F.U. Renner, Y. Gründer, P.F. Lyman, J. Zegenhagen, Thin Sol. Films **2007**, 515, 5574

[26] Z. Liu, P.C. Searson, J. Phys. Chem. B **2006**, 110, 4318

[27] H. Van Swygenhoven, B. Schmitt, P. M. Derlet, S. Van Petegem, A. Cervellino, Z. Budrovic, S. Brandstetter, A. Bollhalder, and M. Schild, Rev. Sci. Instr. **2006**, 77, 013902

[28] N. Tamura, A.A. MacDowell, R. Spolenak, B.C. Valek , J.C. Bravman, W.L. Brown, R.S. Celestre, H.A. Padmore, B.W. Batterman, J.R. Patel, J. Synchrotron Rad. **2003**, 10, 137

[29] J. Biener, A.M. Hodge, A.V. Hamza, Appl. Phys. Lett. **2005**, 87, 121908

[30] C.A. Volkert, E.T. Lilleodden, Phil. Mag. **2006**, 86, 5567

[31] R. Maaß, S. Van Petegem, H. Van Swygenhoven, P.M. Derlet, C.A. Volkert, and D. Grolimund, Phys. Rev. Lett. **2007**, 99, 145505